MEASUREMENT OF THE D-D NEUTRON GENERATION RATE BY PROTON COUNTING

IN JUNG KIM*, NAM SUK JUNG and HEE DONG CHOI
Department of Nuclear Engineering, Seoul National University
San 56-1 Shilim-Dong, Kwanak-Gu, Seoul, 151-744, Republic of Korea
*Corresponding author. E-mail : vandegra@plaza.snu.ac.kr

Received December 26, 2007
Accepted for Publication March 31, 2008

A detection system was set up to measure the neutron generation rate of a recently developed D-D neutron generator. The system is composed of a Si detector, He-3 detector, and electronics for pulse height analysis. The neutron generation rate was measured by counting protons using the Si detector, and the data was crosschecked by counting neutrons with the He-3 detector. The efficiencies of the Si and He-3 detectors were calibrated independently by using a standard alpha particle source ^{241}Am and a bare isotopic neutron source ^{252}Cf, respectively. The effect of the cross-sectional difference between the D(d,p)T and D(d,n)^{3}He reactions was evaluated for the case of a thick target. The neutron generation rate was theoretically corrected for the anisotropic emission of protons and neutrons in the D-D reactions. The attenuations of neutron on the path to the He-3 detector by the target assembly and vacuum flange of the neutron generator were considered by the Monte Carlo method using the MCNP 4C2 code. As a result, the neutron generation rate based on the Si detector measurement was determined with a relative uncertainty of $\pm$5%, and the two rates measured by both detectors corroborated within 20%.

KEYWORDS : D-D Neutron Generator; Neutron Generation Rate Measurement; Proton; Neutron; Anisotropy Correction

1. INTRODUCTION

A D-D neutron generator was recently developed based on large current RF ion source and drive-in Ti target [1]. The current range of the deuteron beam was 0.8 – 8 mA, and the ion beam could be accelerated up to 97.5 keV. It thus achieved a maximum generation rate of 1.9×10^8 n/s during a test-run. In this paper, the method and system used to determine the neutron generation rate of the device is described in detail. Other topics related to the neutron generator, such as design or performance, are reported and discussed in a separate paper [1].

The neutron generation rate was measured by counting protons and crosschecked with the rate measured by direct reading of neutron counting. Typically, the neutron generation rate is measured by counting neutrons using neutron counters or activation detectors [2-4]. However, proton counting [5] is preferable because the efficiency of a proton detector is more accurately defined at a given geometry and the proton peak is easily distinguished from the background spectrum due to its high energy of ~ 3 MeV. Although protons are produced by the D(d,p)T reaction channel while neutrons are produced by the D(d,n)^{3}He reaction channel, they are the products of the same reaction, and the cross sections of both channels are well known. The effect of the cross-sectional difference between the two reaction channels was theoretically evaluated for a thick target, and the effect of the anisotropic emission of the protons and neutrons was corrected.

2. D-D REACTION

2.1 Cross Section

The cross sections of D(d,p)T, D(d,n)^{3}He reactions are shown in Figure 1-(a) according to the ENDF/B-VI data library [6]. The cross section of the D(d,n)^{3}He reaction is slightly larger than that of the D(d,p)T reaction. The cross-sectional difference increased with the rise in energy such that it was approximately 10% at 120 keV. However, the difference between the reaction rates in a thick target was less than the difference of the cross sections due to energy loss of the deuteron beam at the target. Figure 1-(b) illustrates the reaction yields calculated for a thick TiD_2 target according to the incident energy of the deuteron beam. The reaction yields were calculated according to the work of J. Kim [7], and it was assumed that a 100% monatomic deuteron beam was irradiated on the target. The difference between the reaction yields was less than 5% when the incident

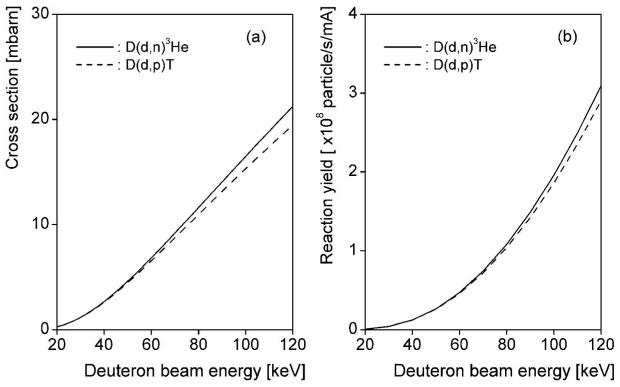

Fig. 1. D(d,p)T and D(d,n)^{3}He (a) Cross Section and (b) Reaction Yield

energy of a deuteron beam did not exceed 100 keV.

2.2 Anisotropy Correction

The emission of protons and neutrons from the D(d,p)T, D(d,n)^{3}He reactions is known to be strongly biased to the forward direction, and the anisotropy increased with the incident energy [8]. The emission anisotropy could, therefore, cause a serious error in determining the neutron generation rate based on a single detector position unless it was taken into consideration. In this study, the emission anisotropy effect on the neutron generation rate measurement was theoretically corrected for the simple case of irradiating a narrow pencil beam on a thick target, as follows.

Let $p(\theta)$ be the probability that a particle produced by a reaction enters a detector with a solid angle of $\Delta\Omega$ at θ in the laboratory system. The $p(\theta)$ was given by,

$$p(\theta,\Delta\Omega)=\frac{\int_0^R dx\int_{\Delta\Omega}d\Omega\left(\left.\frac{d\sigma(\theta')}{d\Omega}\right|_{E(x)}N(x)\right)}{\int_0^R dx[\sigma(E(x))N(x)]} \quad (1)$$

where R was the range of the incident deuteron beam, x was the depth in the target, $d\sigma(\theta')/d\Omega|_{E(x)}$ was a differential cross section at the energy $E(x)$ of the deuteron beam at the depth x, $\sigma(E(x))$ was the cross section at $E(x)$, and $N(x)$ was the number density of deuterium atoms in the target at x. The beam energy $E(x)$ at the target depth x was calculable by using the stopping power code SRIM-2003 [9]. Then an anisotropy correction factor, $f_{A.I.}$, for the particle and detector was given by,

$$f_{A.I.}=\frac{\Delta\Omega/4\pi}{p(\theta,\Delta\Omega)} \quad (2)$$

The generation rate of the particle, G, was given by,

$$G=f_{A.I.}\times\left(\frac{C}{\varepsilon}\right) \quad (3)$$

where C was the measured count rate of the particle and ε was the efficiency of the detector for an isotropic source.

3. MEASUREMENT SYSTEM

The measurement system was constructed, as shown in Figure 2. Specifications of the system components were summarized in Table 1. A Si detector and a He-3 detector were used to count protons and neutrons, respectively. The whole system was electrostatically shielded [10] from intense noises caused by RF waves used to drive the ion source and by spark discharges occurring around the negative biased target during beam irradiation. The measurement of each detection channel was controlled by Gamma Vision [11] and GVU code on a PC platform. Gamma Vision is a commercial program which emulates the MCA (Multi-Channel Analyzer) function. The GVU code is a written routine to help the user to sequentially retrieve spectra in pre-set time intervals and also to monitor the variations using the Gamma Vision program. Detectors were arranged as shown in Figure 3.

The Si detector was 100 μm-thick partially depleted passivated-implanted type. It had an active area of 50 mm^2 and was operated at 40 V. As shown in Figure 3, the detector was placed in the vacuum chamber of the neutron generator at 118° to view the target through a narrow gap between the suppression electrode and the target. The detector was covered with a 40 μm-thick grounded aluminum stopper foil to shield it from the scattered beam, energetic electrons, photons, and leaking RF wave from the ion source. The detection efficiency was defined by placing an aperture of 1.3 mm in diameter before the detector, 112 mm away from the center of the target surface.

The efficiency of the Si detector was calibrated by counting 5.486 MeV alphas from an ^{241}Am standard source with an active area of 5 mm in diameter. This measurements yielded a detector efficiency of 8.6×10^{-6} with a relative uncertainty of ±2%. The different solid angle caused by the larger area of beam irradiation (25 mm in diameter) than that of the ^{241}Am source (5 mm in diameter) was considered by calculation. The calculated efficiency curve according to the source diameter is shown in Figure 4. When the source diameter was 5 mm, the calculated efficiency was consistent with the measured one within the error bar. However, the efficiency calculated for a 25 mm diameter was 3% smaller than the measured efficiency. Hence, a relative uncertainty of ±5% (1σ level) was calculated for the measured efficiency of 8.6×10^{-6}.

The He-3 detector assembly was composed of a He-3 counter tube in a thick polyethylene cylinder to enhance the neutron detection efficiency by counting the slowed

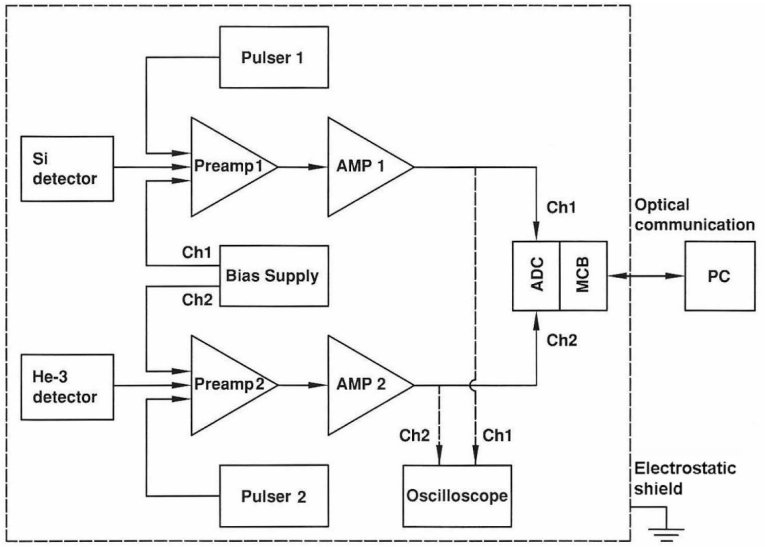

Fig. 2. Block Diagram of the Measurement System

Table 1. Specifications of the Components of the Measurement System

Component	Model	Specifications
Bias supply	710 (ORTEC)	- Voltage range : 0 ~ ±1000 V - Output channel : 4 channels
Preamp 1	142A (ORTEC)	- Input capacitance : 0 ~ 100 pF - Detector bias voltage : 0 ~ ±1000 V
Preamp 2	2006 (CANBERRA)	- Input capacitance : 0 ~ 300 pF - Detector bias voltage : 0 ~ ±2000 V
Amp 1	2020 (CANBERRA)	- Gain : 3 ~ 3900 - Shaping time : 0.25 ~ 12μs
Amp 2	2015A (CANBERRA)	- Gain : 12 ~ 1280 - Shaping time : 0.5 or 2.0 μs
Pulser 1, 2	1407 (CANBERRA)	- Frequency : line or 90 Hz - Rise time : MIN, 20, 50, 100, 250 ns - Fall time : 20, 50, 100, 200, 400 μs
ADC & MCB	919E(ORTEC)	- Fixed conversion time < 7 μs - Memory size : 64k - Input channel : 4 channels

neutrons. As shown in Figure 3, the detector was placed at 0 degrees to the beam direction. On the way to the He-3 detector, a neutron passed at least 80 mm through the polyethylene cylinder, the length of which was about two times the mean free path of a D-D neutron. The periphery of the polyethylene cylinder was covered with a 7 mm thick, borated poly-urethane (9% natural boron) layer to absorb neutrons scattered by surrounding materials before entering the He-3 tube. Physical dimension of the He-3 tube was 25 mm (diameter) ×255 mm (length) and the length of the active volume was 150 mm. The detector was operated at 950 V.

The efficiency of the He-3 detector assembly was measured using a bare standard ^{252}Cf source at the KAERI (Korea Atomic Energy Research Institute). The measurement was performed in a hall of 8 m(L) × 6 m(W) × 6 m(H) by varying the source-to-detector distance between 300 and 1500 mm. In the He-3 detector signal

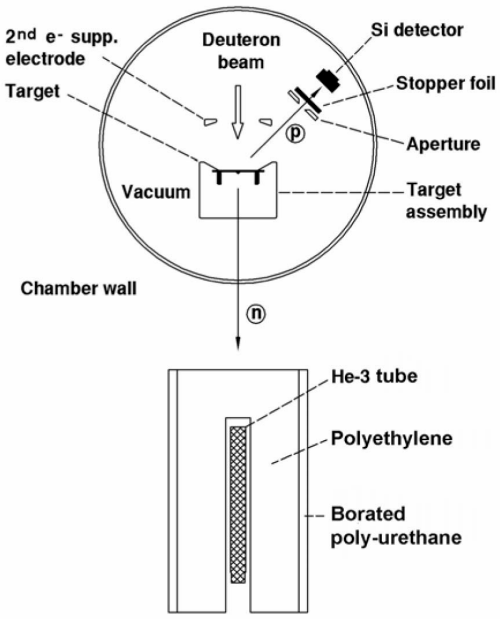

Fig. 3. Schematics of the Detector Arrangement

spectrum, some counts of gamma-ray induced signals were also observed. These signals were easily discriminated since the pulse height of gamma-ray induced signals was much smaller than that of neutron induced signals. The measured efficiency at long source-to-detector distances became less accurate because the scattered neutrons contributed more to the neutron count. This contribution of the scattered neutrons was evaluated using the MCNP 4C2 code [12,13]. The simulation showed that neutron flux in the detector volume doubled at 1500 mm due to the contribution of scattered neutrons. Therefore, the He-3 detector was positioned as close to the neutron generator target as possible, at 330 mm where the measured efficiency was 8.0×10^{-5} with a relative uncertainty of ±5%. The discrepancy between the neutron source spectrum from the ^{252}Cf isotopic source and the D-D reaction was not considered as most of the neutrons must have slowed in the thick polyethylene cylinder.

4. EXPERIMENTAL RESULTS

The proton energy spectrum measured by the Si detector was as shown in Figure 5. The proton was emitted at ~3 MeV from the D-D reaction at 118° in laboratory system, and it lost ~1 MeV at the stopper foil. Here the energy loss at the stopper foil was calculated by using the stopping power code SRIM-2003 [9]. Hence, the proton peak was detected at ~1.8 MeV, as shown in the figure. The peak width was somewhat broadened by the noise signals and the energy loss stragglings at the target and stopper foil. Neither triton nor ^{3}He from the D(d,p)T, D(d,n)^{3}He reactions were observed in the spectrum due to blocking at the stopper foil. Another peak appeared in the higher energy region (> 6,000 channel) due to a reference pulse signal, and some counts recorded in the low energy region (< 1,000 channel) were due to the noise signals. Despite the width of the proton peak, approximately 140 keV FWHM (Full Width at Half Maximum), there was little interference and negligible background. The gross count under the proton peak was regarded as the proton count.

By using the measured proton count rate, the neutron generation rate was determined with corrections for the cross-sectional difference of the D(d,p)T, D(d,n)^{3}He reactions and for the anisotropic emission of protons. The effect of the cross-sectional difference was corrected using

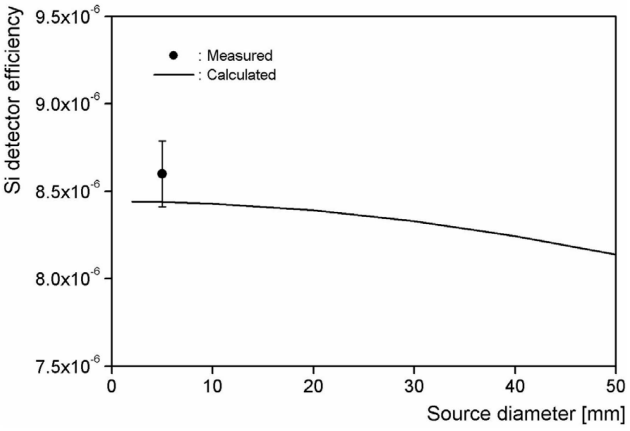

Fig. 4. The Measured and Calculated Efficiency of the Si Detector

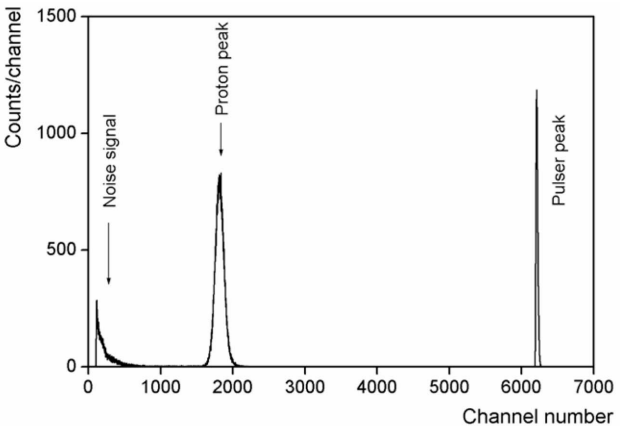

Fig. 5. Proton Energy Spectrum Measured by the Si Detector (Peak Center: 1.8 MeV, FWHM: 140 keV)

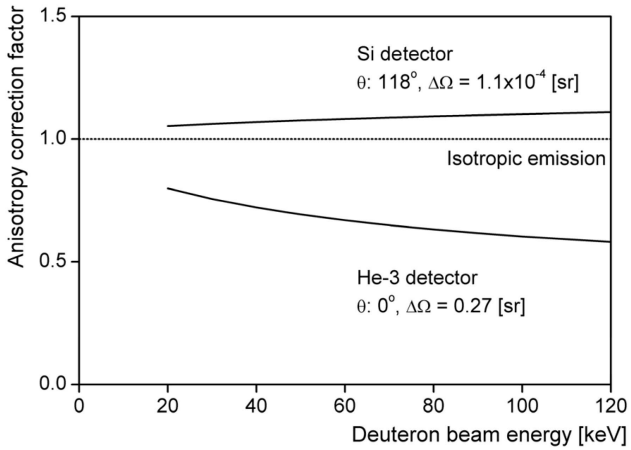

Fig. 6. Anisotropy Correction Factor Curves for the Detectors

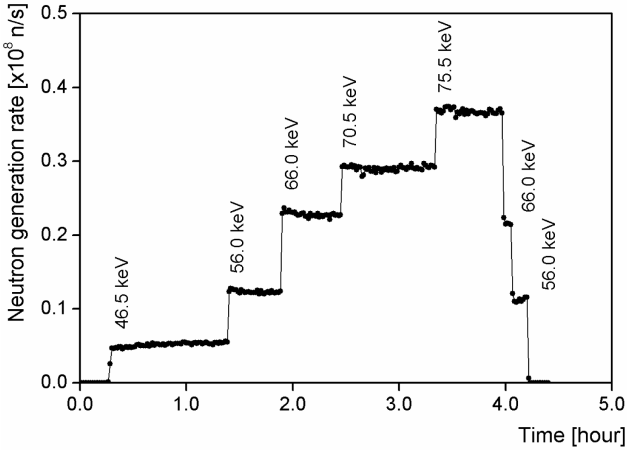

Fig. 7. Neutron Generation Rate Measured by the Si Detector During a Neutron Generation Run (Deuteron Beam Current: 3.9 mA)

the ratio of the calculated reaction yields in Figure 1. The anisotropy correction factor, $f_{A.I.}$, was calculated according to Eq. (2), and the angular distribution coefficients measured by Krauss *et al*. [8] were used for the calculation. The calculated anisotropy correction factor for the Si detector is shown in Figure 6. The neutron generation rate measured with the Si detector is shown in Figure 7. The beam energy increased stepwise from 46.5 keV to 75.5 keV, and the rate was measured every minute. A neutron generation rate of 3.8×10^7 n/s was measured at 75.5 keV and at 3.9 mA of total beam current with a relative uncertainty of ±5%. The uncertainty was propagated from the efficiency calibration uncertainty of the Si detector and the statistical uncertainty of the proton count. Here the neutron yield was one order of magnitude lower than the one predicted by the Figure 1. Two factors were considered to attribute the low neutron yield: (1) the monatomic fraction of the deuteron beam, (2) the loaded amount of the deuteron target nuclei and the shape of concentration profile [1].

The neutron generation rate was measured in parallel by the He-3 detector during the test run. The measured signal spectrum of the He-3 detector by the D-D neutrons from the neutron generator is shown in Figure 8. The reaction product full-energy peak of the ^{3}He(n,p)T reaction (0.764 MeV) was increased at 1500 channel, and the wall effect [14] was recorded as continuums at lower channel. No gamma-ray induced signals which appeared in ^{252}Cf-neutron measurement were counted in the detector signal spectrum. The gamma-ray field was considered to be less intense than in the ^{252}Cf-neutron measurement environment since the ^{252}Cf source itself was a strong gamma-ray emitter [15]. Hence, the gross count within a range of 360 - 1500 channels was regarded as a neutron count. The neutron generation rate was also corrected for the anisotropic emission of neutrons and attenuation of the neutron flux at the structural materials of the neutron generator. The calculated anisotropy correction factor for the He-3 detector is shown in Figure 7. The attenuation correction factor was calculated using the MCNP 4C2 code [12,13] by comparing the neutron flux calculated with and without the target assembly and vacuum flange of the neutron generator. The attenuation correction factor was 1.73 with a statistical uncertainty of ±1% (1σ level). The effect of additional neutrons from the D-T reaction as a byproduct of the D(d,p)T reaction was ignored because the contribution would not exceed approximately 1% [16].

Figure 9 shows the comparisons between the two rates measured by the detectors. The x-axis was the rate measured by the Si detector, and the y-axis was the rate measured by the He-3 detector. The open square was the rate obtained with no anisotropy correction. Due to the strong bias of neutron emission to the forward direction,

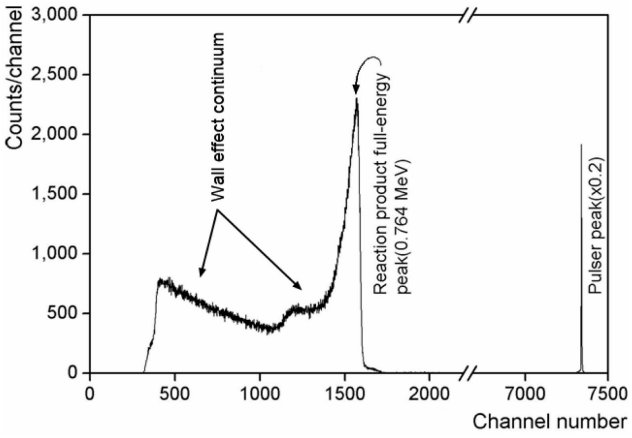

Fig. 8. Signal Spectrum of the He-3 Detector by the D-D Neutron

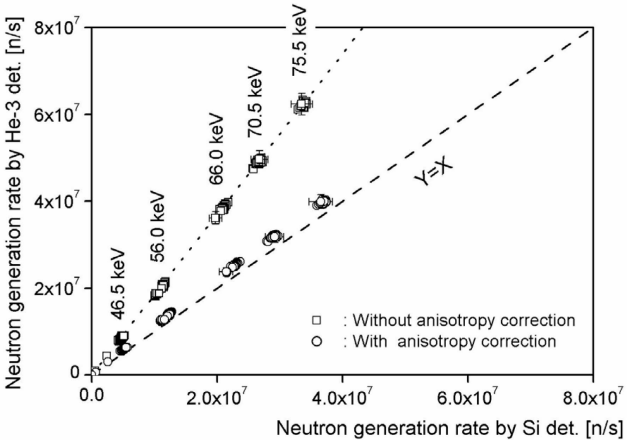

Fig. 9. Neutron Generation Rates Measured by the Si and He-3 Detectors

the rate measured by the He-3 detector at 0 degrees was overestimated by as much as a factor of two. The open circle was the rate after the anisotropy correction, indicating a stronger agreement between the detectors. Although the He-3 detector recorded a slightly higher rate than the Si detector, the rates agreed within about 20%. The detection discrepancy of 20% was due to neutrons scattered by surrounding materials as the measurement was performed in a small enclosure surrounded by heavy shielding blocks.

5. CONCLUSIONS

A detection system was set-up to reliably measure the neutron generation rate of a recently developed D-D neutron generator [1], composed of a Si and a He-3 detector which were used to count protons and neutrons, respectively. The neutron generation rate was primarily measured with the Si detector. The rate was theoretically corrected for the cross-sectional difference between the D(d,p)T, D(d,n)^{3}He reactions and for the anisotropic emission of the proton. As a result, the neutron generation rate was measured with the Si detector with a relative uncertainty as low as ±5%. The rate measured by the Si detector was crosschecked by counting neutrons. The He-3 detector calibrated with a ^{252}Cf isotopic neutron source was used, and the rate was theoretically corrected for the anisotropic emission of neutrons and for the attenuation of neutrons at the structure materials of the neutron generator. The consideration of anisotropic emission of D-D neutrons was crucial to understand the apparent difference between the simple readings of the two detectors. The He-3 detector reading was slightly higher (approximately 20%) than that of the Si detector, which was due to the neutrons scattered by the surrounding materials. Therefore, the present study indicates that an accurate D-D neutron measurement is fairly complex when an environment filled with device structures and components is taken into account.

ACKNOWLEDGEMENTS

This research was performed under a program of the Basic Atomic Energy Research Institute (BAERI), which is a part of the Nuclear R&D Programs funded by the Ministry of Science & Technology (MOST) of South Korea. We would like to give thanks to Dr. Bong Hwan Kim at KAERI for allowing use of the ^{252}Cf isotopic neutron source and related equipment for the efficiency calibration of the He-3 detector.

REFERENCES

[1] I.J. Kim, N.S. Jung, H.D. Jung, Y.S. Hwang and H.D. Choi, "A D-D Neutron Generator Using a Titanium Drive-in Target", *Nucl. Instr. and Meth. B*, **266**, 829 (2008).
[2] R.L. Hirsch, "Inertial-Electrostatic Confinement of Ionized Fusion Gases", *J. Appl. Phys*., **38**, 4522 (1967).
[3] G.H. Miley and J. Sved, "The IEC-A Plasma-target-based Neutron Source", *Appl. Radiat. and Isot*., **48**, 1557 (1997).
[4] J. Reijonen, "Neutron Generators Developed at LBNL for Homeland Security and Imaging Applications", *Nucl. Instr. and Meth. B*, **261**, 272 (2007).
[5] J. Csikai, *CRC Handbook of Fast Neutron Generators*, Vol. 1, p. 99, CRC Press, Inc., Florida (1987).
[6] Cross Section Evaluation Working Group, "ENDF/B-VI Summary Documentation", Report BNL-NCS-17541 (ENDF-201), P.R. Rose (Ed.), National Nuclear Data Center, Brookhaven National Laboratory (1991).
[7] J. Kim, "Neutron Sources Using D-T Mixed Beams Driven into Solid Target", *Nucl. Instr. and Meth*., **145**, 9 (1977).
[8] A. Krauss, H.W. Becker, H.P. Trautvetter, C. Rolfs and K. Brand, "Low-Energy Fusion Cross Sections of D+D and D+^{3}He Reactions", *Nucl. Phys. A*, **465**, 150 (1987).
[9] J.F. Ziegler, "SRIM-2003", *Nucl. Instr. and Meth. B*, **219-220**, 1027 (2003).
[10] R. Morrison, *Grounding and Shielding Techniques in Instrumentation*, **3rd Ed**., John Wiley & Sons, New York (1986).
[11] ORTEC, "Gamma Vision® 32: Gamma-ray Spectrum Analysis and MCA Emulator for Microsoft® Windows® 95, 98, 2000, and NT®", A66-B32 Software User's Manual, Software Version 5.3, USA.
[12] J.F. Briesmeister(Ed), "MCNP – a General Monte Carlo N-particle Transport Code, Version 4C", LA-13709-M, Los Alamos National Laboratory (2000).
[13] J.S. Hendricks, "MCNP4C2", X-5:RN(U)-JSH-01-01, Memorandum, Los Alamos National Laboratory (2001).
[14] G.F. Knoll, *Radiation Detection and Measurement*, **2nd Ed**., p. 481, John Wiley & Sons, New York (1989).
[15] H.H. Barschall, in: A. Michaudon, S. Cierjacks, R.E. Chrien(Eds.), *Neutron Sources for Basic Physics and Applications*, p. 7, Pergamon Press Ltd., Oxford, 1983.
[16] F.E. Cecil and E.B. Nieschmidt, "Production of 14 MeV Neutrons from D-D Neutron Generators", *Nucl. Instr. and Meth. B*, **16**, 88 (1986).